Actin-bundling protein L-plastin promotes megakaryocyte rigidity and dampens proplatelet formation

Normal hemostasis requires an adequate number of normally functioning platelets. A better understanding of platelet biogenesis may facilitate the expanding effort to manufacture platelets *in vitro*.[1] Platelets develop from mature bone marrow megakaryocytes (MK) that derive from megakaryocyte progenitor (MKP) cells.[2] In the classic model of bone marrow megakaryopoiesis, hematopoietic stem cells (HSC) in the proliferative niche give rise to MK-erythroid progenitors that differentiate into MKP during migration to the vascular nice.[3] The cytoplasm of mature MK has an abundant invaginated membrane system (IMS) that is contiguous with the plasma membrane.[4,5] During the late stages of thrombopoiesis, the IMS begins extrude from the MK plasma membrane and form long extensions of proplatelets (PP) that eventually give rise to platelets released in the vasculature.[6,7] Cell migration and signaling requires alterations in the organization and thickness of the cell cortex, which is comprised of a network of overlapping, bundled and crosslinked actin filaments.[8] Filamentous actin (F-actin) organization regulates MK shape, MKP migration, formation of the IMS, early stage of PP formation (PPF), and later stages of PP branching. Despite this understanding of various stages of MK differentiation, the molecular mechanisms that signal the MK to initiate PPF are not well understood.

Recently, our laboratory used an unbiased transcriptomic approach to identify an actin bundling protein, L-plastin, that decreased during MK differentiation, correlating with the onset of PPF.[9] Using CRISPR/Cas to generate $CD34^+$-derived human MK deficient in L-plastin, we found impaired MK migration in response to SDF-1α chemoattractant, increased podosome formation per MK, increased IMS and increased PPF. F-actin polymerization and depolymerization (i.e., "re-organization") are dynamic reactions central to MK shape, migration, IMS formation, etc. F-actin also facilitates degradation of the extracellular matrix at sites of podosome formation.[10] The MK cytoskeleton, comprised of a dense network of actin filaments and microtubules, is located at the periphery of the cell cytoplasm, below the plasma membrane. The manner by which the loose lipid-rich IMS is able to penetrate the dense actin cytoskeleton to initiate PPF has not been addressed. The prior work on MK L-plastin was limited by inter-individual variation affecting platelet number and artifacts of *in vitro* culturing.[9] Because MK L-plastin has not been studied *in vivo*, and because L-plastin is expected to increase the density of the MK actin cortex via actin bundling, we used L-plastin-deficient mice[11] to assess the effects of L-plastin on *in vivo* hemostasis and thrombosis, determine the intracellular location of MK L-plastin, and assess MK membrane rigidity. We report that MK L-plastin colocalizes with actin in wild-type MK, and loss of MK L-plastin reduces MK membrane rigidity and increases MK PPF, providing a novel mechanism for regulating platelet formation.

We first confirmed L-plastin protein expression in platelets from wild-type mice and littermate knockout mice with a disrupted *Lcp1* gene lacked platelet L-plastin protein (*Online Supplementary Figure S1A*). Initial experiments addressed the effect of *in vivo* L-plastin deficiency on screening assays for hemostasis and thrombosis. Tail bleeding times and survival times after a pulmonary embolism model were shorter in L-plastin expression mice (Figure 1A, B), suggesting a prothrombotic phenotype in the knockout animals. Although this mouse strain is a global knockout, L-plastin expressionis limited to hematopoietic cells, and prior studies have focused on L-plastin effects in leukocytes.[12] We, therefore, sought to investigate the role of L-plastin in thrombopoiesis using the L-plastin-deficient mice. Compared to wild-type mice, peripheral blood platelet counts in *Lcp1*$^{-/-}$ mice were modestly but significantly higher, with no difference in mean platelet volume (Figure 1C, D). Under steady state conditions and compared to wild-type mice, *Lcp1*$^{-/-}$ mice have normal red blood cell counts and modestly increased white blood cell counts (*Online Supplementary Figure S1B, C*), but no differences in body weight. Both male and female mice were studied and no effect of sex on the platelet count difference was observed. Note that the comparisons in this study were between inbred strains of *Lcp1* wild-type and *Lcp1*$^{-/-}$ littermates, so we would not expect environmental or other genetic confounding factors. These *in vivo* data support the use of this *Lcp1*$^{-/-}$ mouse line for studies of L-plastin in the MK/platelet lineage.

No difference was observed between the number of acetylcholinesterase-positive MK in wild-type and *Lcp1*$^{-/-}$ mice (*Online Supplementary Figure S2*), suggesting L-plastin may not affect megakaryopoiesis. However, compared to wild-type mice, *Lcp1*$^{-/-}$mice had significantly more PP-forming MK (Figure 2A, B), consistent with an inhibitory role of L-plastin in platelet production.[9] We examined the subcellular distribution of L-

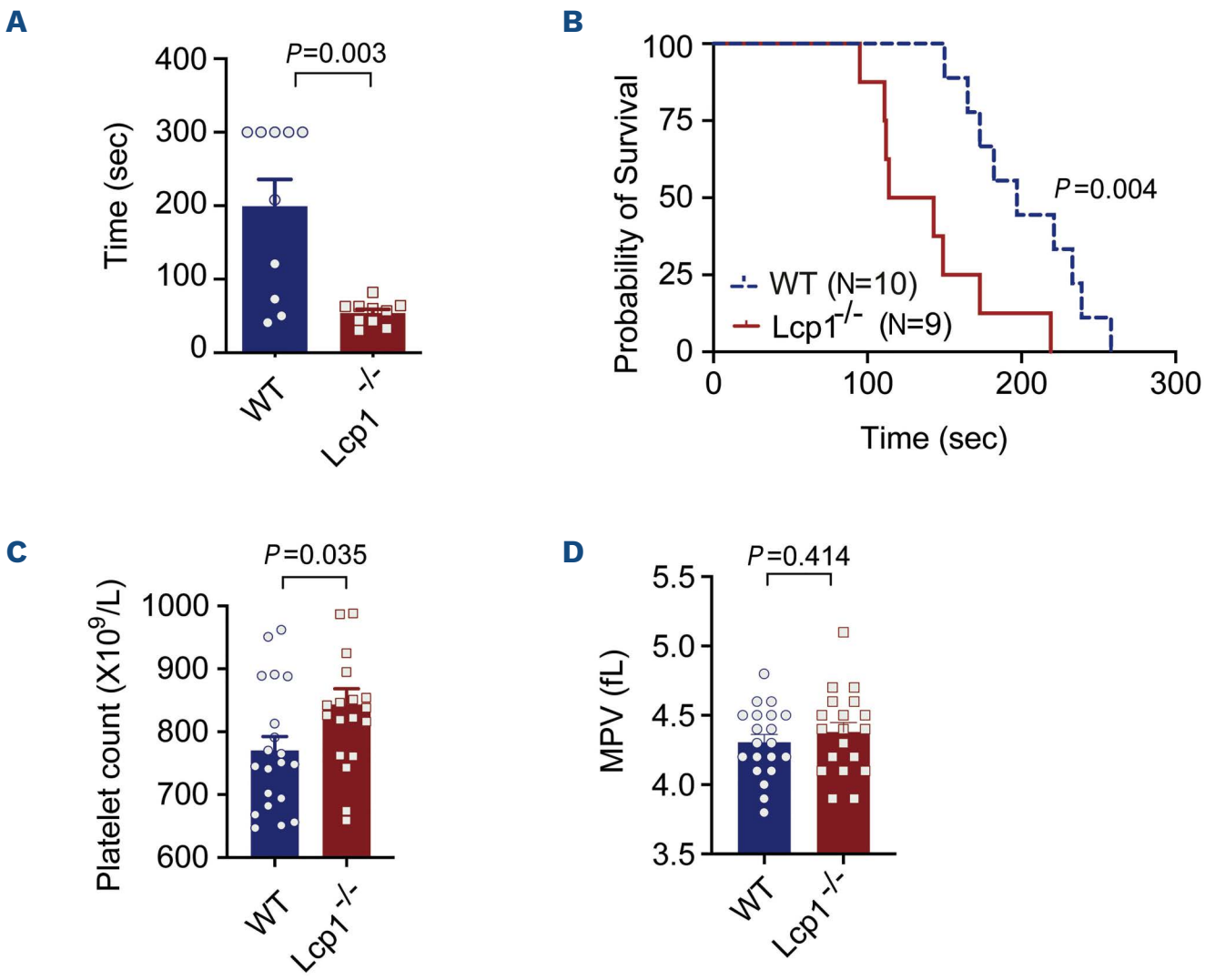

Figure 1. *In vivo* hemostasis and thrombosis models. (A) Tail-bleeding time for wild-type (WT) *Lcp1*$^{+/+}$ and *Lcp1*$^{-/-}$ littermate mice (*Lcp1*$^{+/+}$ N=10, *Lcp1*$^{-/-}$ N=10). (B) Pulmonary thromboembolism was induced by injecting *Lcp1*$^{+/+}$ or *Lcp1*$^{-/-}$ mice with collagen and epinephrine. Time to death was monitored and plotted (*Lcp1*$^{+/+}$ N=10, *Lcp1*$^{-/-}$ N=9). (C) Platelet count and (D) mean platelet volume (MPV) in the peripheral blood from littermate *Lcp1*$^{+/+}$ and *Lcp1*$^{-/-}$ mice of both sexes. Each dot/circle is an individual mouse (N=19-20).

plastin in MK using immunofluorescent confocal microscopy. Figure 2C demonstrates co-localization between L-plastin and F-actin in MK adherent to both poly-L-lysine and fibrinogen. A prominent distribution of L-plastin was observed below the plasma membrane of MK. Similar results were obtained with human CD34^{+}-derived MK (*Online Supplementary Figure S3*). Taken together, these data suggest a hypothesis whereby L-plastin-mediated F-actin bundling results in a denser MK actin cortex that impedes the IMS protrusion necessary to initiate PPF. However, we cannot exclude an increase in lifespan as an additional contributor to the increased platelet count in the *Lcp1*$^{-/-}$ mice.

We have previously shown that L-plastin expression decreases with MK maturation.[9] A corollary of the above hypothesis is that lower levels of L-plastin in mature MK cause reduced actin bundling and hence, a less stiff MK actin cytoskeleton. Because integral membrane proteins directly or indirectly attach the plasma membrane to the outermost layer of actin filaments of the cortical cytoskeleton,[13] we tested this corollary by measuring MK cytoskeleton stiffness using the Biomembrane Force Probe (BFP) tether assay (illustrated in Figure 3A, B).[14,15] Compared to wild-type MK, L-plastin-deficient MK were significantly less rigid (Figure 3C). Lastly, we used CRISPR to knockdown expression in cultured human MK and observed a similar relationship between L-plastin and membrane rigidity (Figure 3D).

The molecular switches that tell the mature MK to begin PPF are incompletely understood. Actin, myosin heavy and light chains, tubulin, kinases, and phosphatases are all critical for this process. Bury *et al*. have reviewed inherited causes of thrombocytopenia, and listed 11 genes that regulate PPF.[16] Based on the rationale that changes in gene expression during MK differentiation might provide clues to genes regulating normal PPF, we previously performed RNA sequencing on biologic replicates of day 6, day 9 and day 13 cord blood-differentiated Mk,[9] and found numerous candidate genes, most of which increased as MK began to form PP. Like ROCK1,[17] L-plastin is one of the few inhibitors of PPF described to date.

In summary, we measured MK cytoskeleton stiffness for the first time and found an important role of the actin cytoskeleton stiffness in PPF. We showed that i) mice deficient in the actin-bundling protein L-plastin have an increased MK PPF and higher platelet counts,

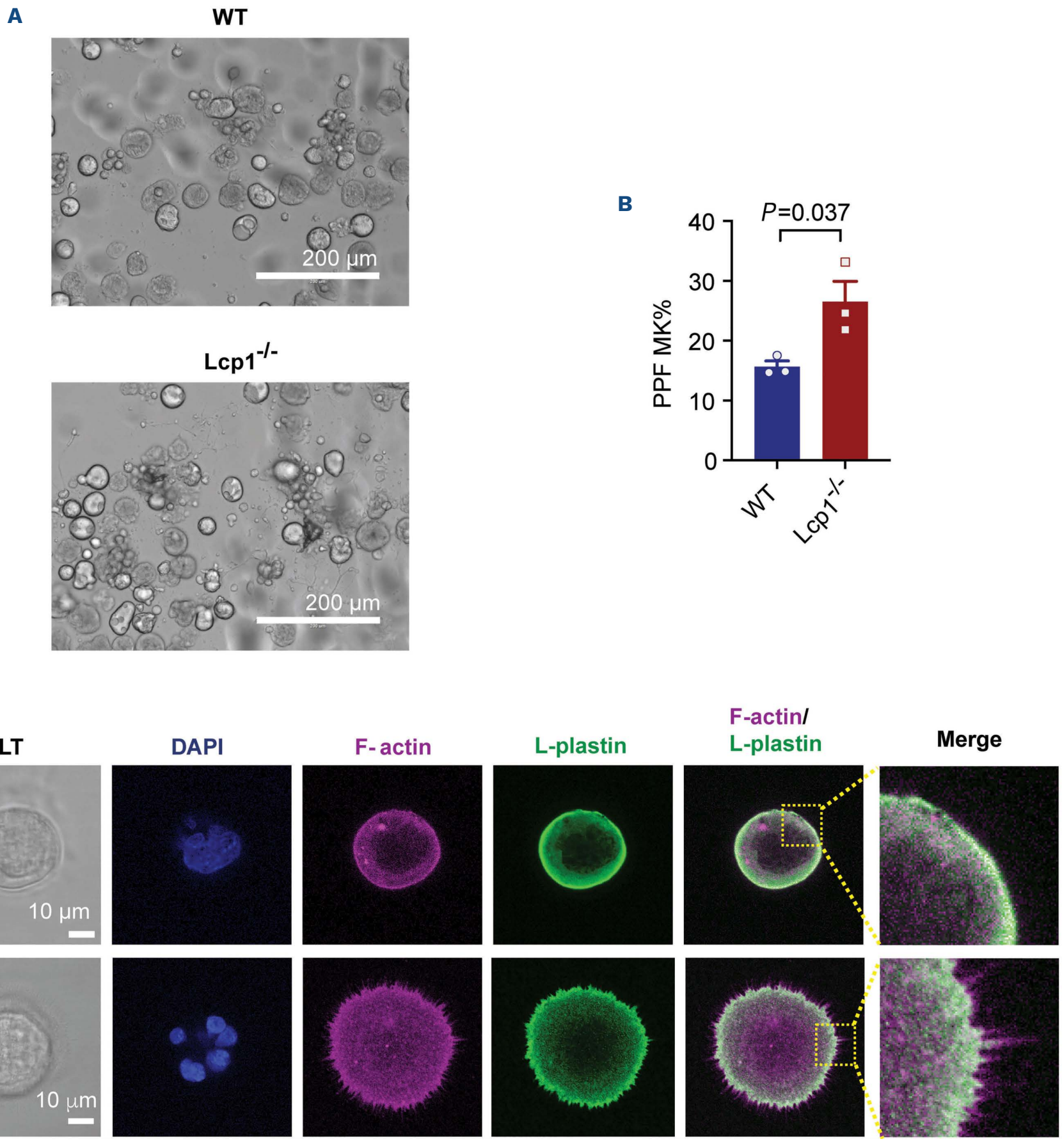

Figure 2. L-plastin inhibits megakaryocyte proplatelet formation and localizes with F-actin. (A) Representative images of megakaryocyte (MK)-forming proplatelets (PP) from both *Lcp1*$^{+/+}$ and *Lcp1*$^{-/-}$ mice. Mouse bone marrow cells were stimulated with 50 ng/mL thrombopoietin for 3-4 days. MK were enriched using bovine serum albumin gradient and cultured for another 16-24 hours and examined by light transmission (LT) microscopy. (B) Quantification of PP-forming MK. PP-forming MK were defined by at least 1 filamentous pseudopod observed by light microscopy with a 20x objective of day 3-4 cultured cells. Scoring was blinded as to *Lcp1* genotype, and the percent of total MK number plotted. Three or more images from each of 3 pairs of littermates *Lcp1*$^{+/+}$ and *Lcp1*$^{-/-}$ mice were counted and the average percentage per mouse was plotted. (C) Representative immunofluorescent confocal images of C57BL/6 MK stained for DNA (DAPI), F-actin (magenta) and L-plastin (green). F-actin/L-plastin co-localization is white. MK seeded on poly-L-lysine (PLL) or fibrinogen (FGN). PPF: proplatelet formation.

and ii) mouse and human MK L-plastin levels strongly correlate with MK membrane rigidity. Since higher MK membrane rigidity likely correlates with actin cytoskeletal density, higher levels of L-plastin in immature MK could prevent premature release of platelets in the bone marrow. At the mature stage of MK differentiation, L-plastin levels have decreased, which is expected to reduce actin bundling and actin cytoskeletal rigidity, and facilitate initiation of membrane PP protrusions (Figure 3E). Bisaria *et al*. recently showed that newly

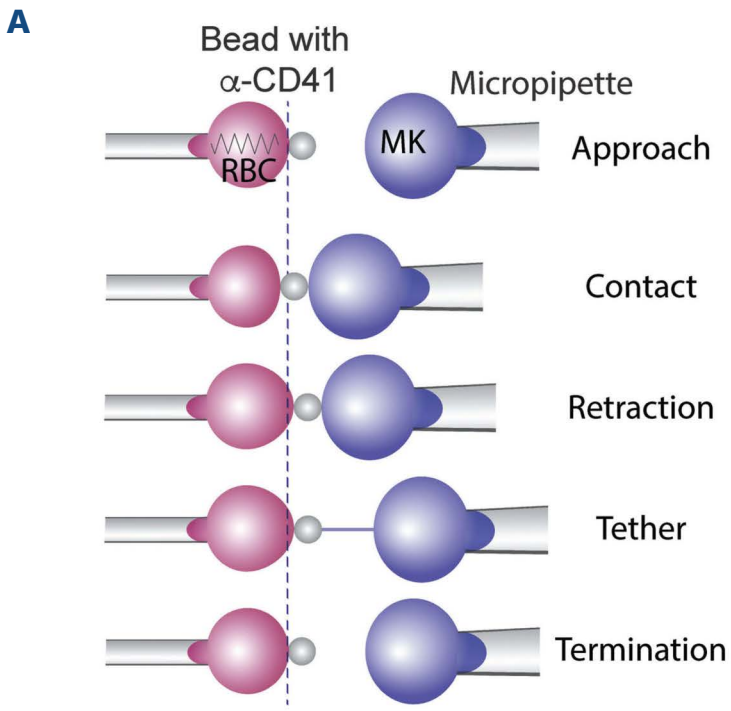

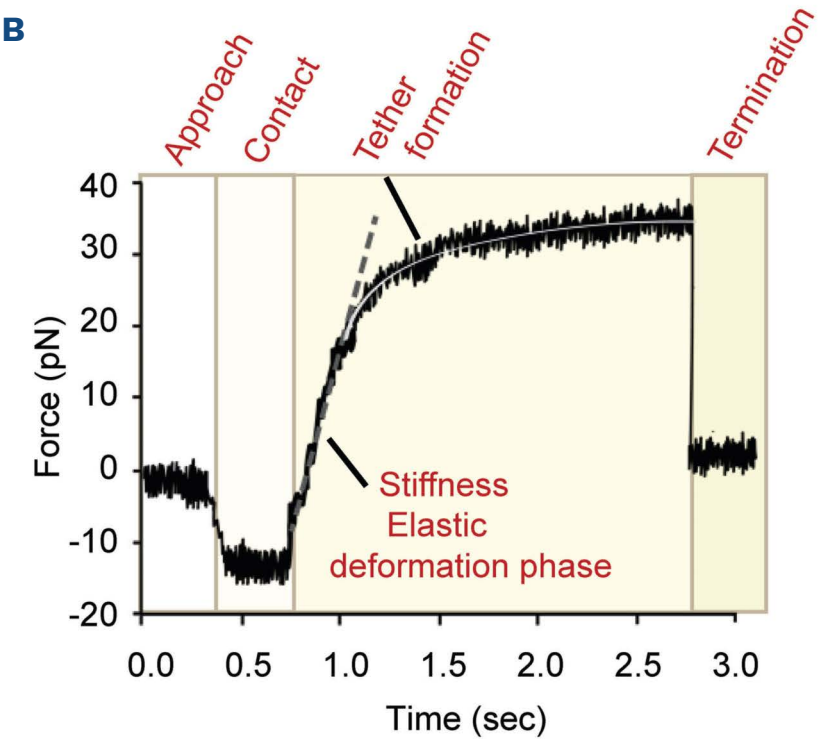

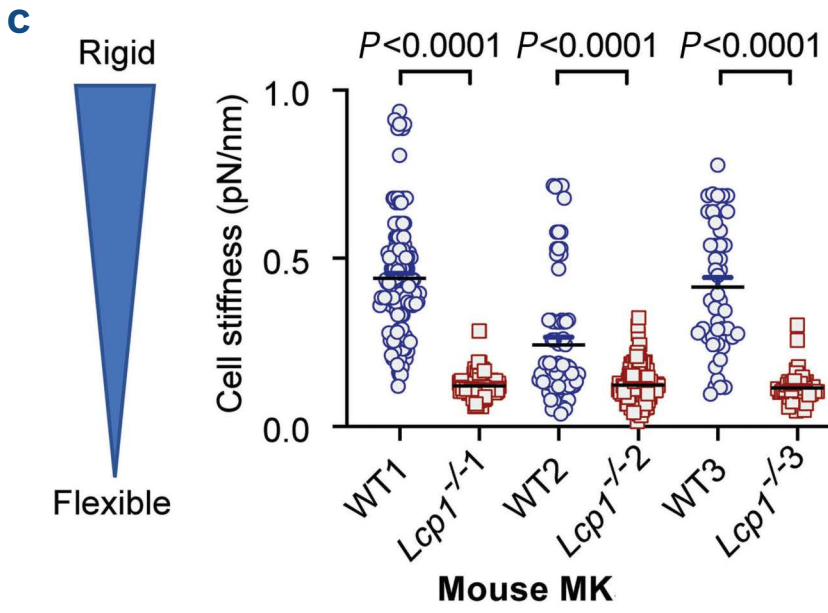

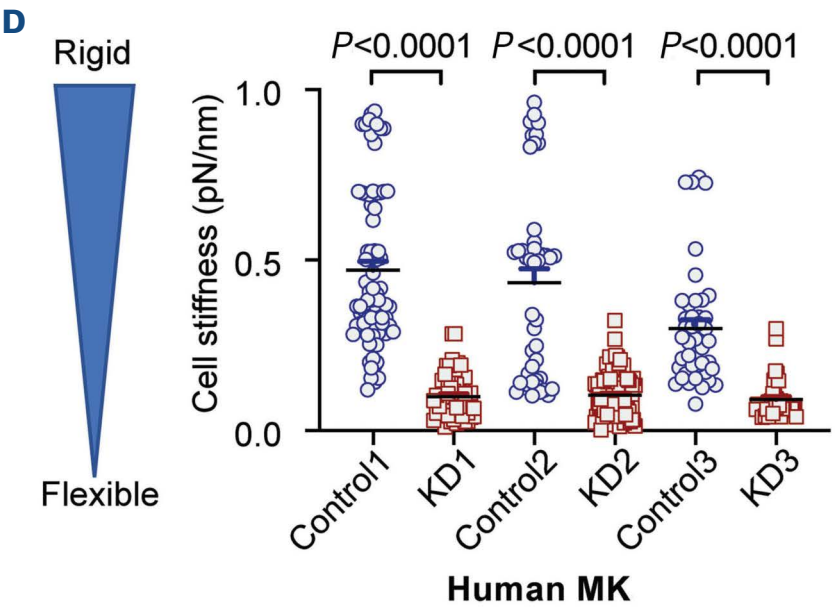

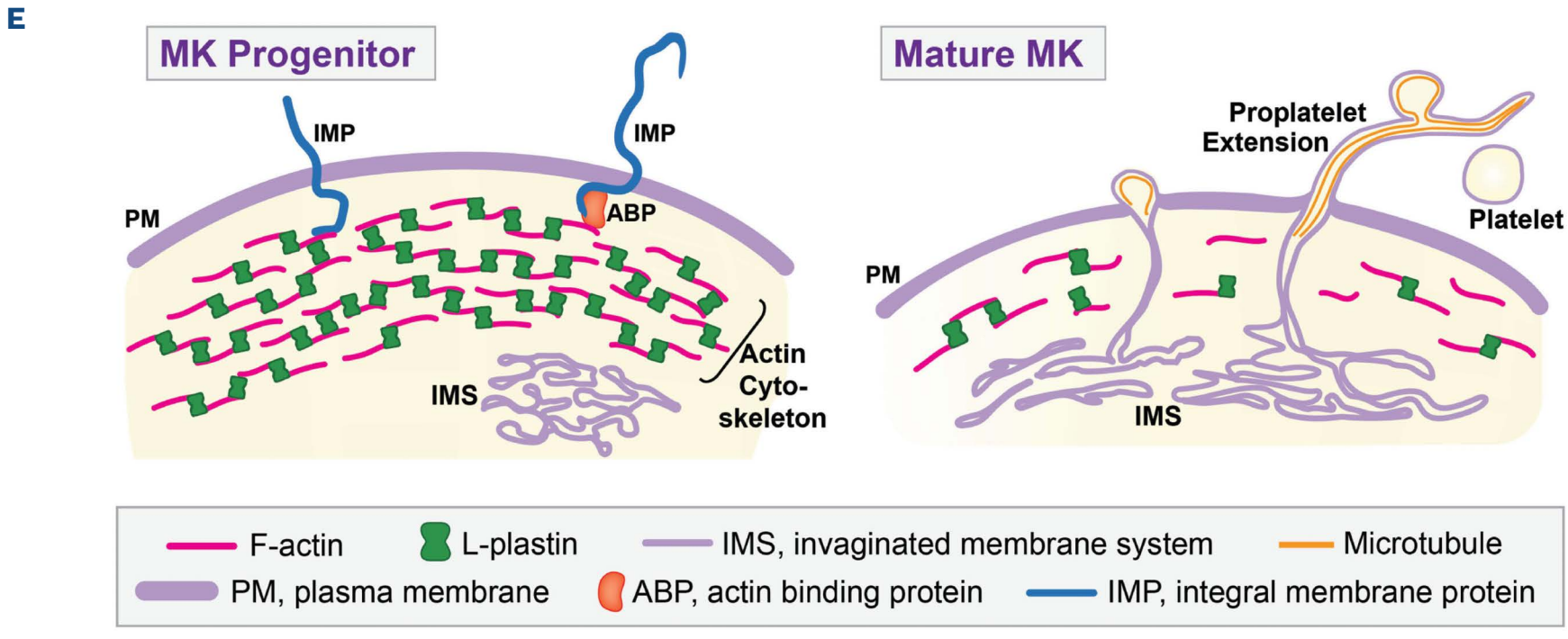

Continued on following page.

Figure 3. L-plastin maintains megakaryocyte membrane stiffness. (A) Illustration of the Biomembrane Force Probe (BFP) tether assay for the measurement of cell stiffness. Borosilicate beads labeled with mouse anti-CD41 antibody were attached to the apex of red blood cell (RBC) at the tip of a micropipette (left). A single megakaryocyte (MK) held by a micropipette (right) approaches the antibody-coated beads and is allowed to attach. Once attached, the MK pipette is pulled back under a constant speed. The cell stiffness is calculated using the pulling force required (= the elastic deformation phase). (B) Representative BFP tether assay readout plot. During the initial approaching stage, no force was detected. During the contact phase, the MK squeezes the bead and shows negative force. During the retraction phase, force is rapidly generated in the linear elastic deformation phase. Cell stiffness was calculated from the elastic deformation phase using the customized package run by LabVIEW (National Instruments). The experiment terminates when the MK detaches from the anti-CD41 coated bead. (C) The BFP tether assay MK membrane stiffness in pico-Newtons (pN) per nanometer (nm) for 3 pairs of mice (wild-type [WT] 1-3 and *Lcp1*$^{-/-}$ 1-3). Each circle represents a single MK. (D) Similar to panel (C), the BFP tether assay was used to assess human MK membrane rigidity in CD34^{+}-derived MK treated without (control 1-3) and with (knockout [KD] 1-3) CRISPR-mediated knockdown of L-plastin. N=3 pairs of different cord blood donor cells.

forming lamellipodial protrusions form in areas of low membrane proximal F-actin density,[18] and it will be of interest for future studies to assess the effect of L-plastin-mediated actin bundling on the ability of cofilin to depolymerize F-actin.

Authors

Li Guo,[1-4] Shancy Jacob,[1] Bhanu Kanth Manne,[1] E. Motunrayo Kolawole,[5] Siqi Guo,[1,6] Xiang Wang,[7] Darian Murray,[1] Emilia A. Tugolukova,[1] Irina Portier,[1] Yasuhiro Kosaka,[1] Cindy Barba,[5] Matthew T. Rondina,[1,5,8,9] Brian Evavold,[5] Celeste Morley,[10,11] Seema Bhatlekar[1#] and Paul F. Bray[1,2#]

[1]Program in Molecular Medicine, Department of Internal Medicine, University of Utah, Salt Lake City, UT; [2]Division of Hematology and Hematologic Malignancies, Department of Internal Medicine, University of Utah, Salt Lake City, UT; [3]Bloodworks Research Institute, Seattle, WA; [4]Hematology Division, University of Washington, Seattle, WA; [5]Department of Pathology, University of Utah, Salt Lake City, UT; [6]Applied Mathematics, Department of Mathematics, University of Utah, Salt Lake City, UT; [7]HSC Cell Imaging Core, School of Medicine, University of Utah, Salt Lake City, UT; [8]Department of Internal Medicine, University of Utah, Salt Lake City, UT; [9]George E. Wahlen Department of Veterans Affairs Medical Center, Department of Internal Medicine, and Geriatric Research, Education, and Clinical Center (GRECC), Salt Lake City, UT; [10]Pediatrics, Infectious Diseases, Washington University, St. Louis, MO and [11]Pathology and Immunology, Washington University, St. Louis, MO, USA

[#]SB and PFB contributed equally as senior authors.

Correspondence:
P. F. BRAY - Paul.bray@hsc.utah.edu
S. BHATLEKAR - saseems@gmail.com

https://doi.org/10.3324/haematol.2023.283016

Received: February 24, 2023.
Accepted: July 6, 2023.

Early view: July 13, 2023.

Disclosures

No conflicts of interest to disclose.

Contributions

LG, SJ, BKM, EKM, SG, XW, DM, EAT, IP, YK, CB and SB performed research. LG, SB and PFB wrote the manuscript. MTR, BE and CM provided scientific expertise.

Acknowledgments

The authors wish to acknowledge experiment technical support from Jesse W. Rowley, Frederik Denorme, Mark J. Cody, Neal D. Tolley, Marina Tristao and Meenakshi Banerjee, editorial help from Neal D. Tolley, and figure preparation expertise from Diana Lim and Nikita Abraham, Molecular Medicine Program, University of Utah, as well as the technical support from Xue Lin, Washington University in St. Louis.

Funding

This study was supported by grants from the National Institutes of Health (R01HL141424, K24HL155856, R01HL142804, R01AG048022, R56AG059877, and R01HL130541, R01AI169835, R01AI104732,) and the Division of Hematology and Hematologic Malignancies at the University of Utah. This work was also supported by Merit Review Award Number I01 CX001696 from the US Department of Veterans Affairs Clinical Sciences R&D (CSRD). In addition, this work was supported by American Heart Association Career Development Award (No. 938717 to LG) and American Heart Association Postdoctoral Fellowship (2022Post906231 to IP). This material is the result of work supported with resources at the George E. Wahlen VA Medical Center, Salt Lake City, Utah. The contents do not represent the views of the US Department of Veterans Affairs or the United States Government. The authors thank the University of Utah Flow Cytometry Facility in addition to the National Cancer Institute through Award No. 5P30CA042014-24.

Data-sharing statement

The data and experimental protocol are available upon request.

References

1. Chen SJ, Sugimoto N, Eto K. Ex vivo manufacturing of platelets: beyond the first-in-human clinical trial using autologous iPSC-platelets. Int J Hematol. 2023;117(3):349-355.
2. Machlus KR, Italiano JE Jr. Megakaryocyte development and platelet formation. In: Michelson AD, editor. Platelets. 4th ed. London, UK. Academic Press; 2019. Chapter 2; p. 25-46.
3. Woolthuis CM, Park CY. Hematopoietic stem/progenitor cell commitment to the megakaryocyte lineage. Blood. 2016;127(10):1242-1248.
4. Eckly A, Heijnen H, Pertuy F, et al. Biogenesis of the demarcation membrane system (DMS) in megakaryocytes. Blood. 2014;123(6):921-930.
5. Antkowiak A, Viaud J, Severin S, et al. Cdc42-dependent F-actin dynamics drive structuration of the demarcation membrane system in megakaryocytes. J Thromb Haemost. 2016;14(6):1268-1284.
6. Hamada T, Mohle R, Hesselgesser J, et al. Transendothelial migration of megakaryocytes in response to stromal cell-derived factor 1 (SDF-1) enhances platelet formation. J Exp Med. 1998;188(3):539-548.
7. Eckly A, Scandola C, Oprescu A, et al. Megakaryocytes use in vivo podosome-like structures working collectively to penetrate the endothelial barrier of bone marrow sinusoids. J Thromb Haemost. 2020;18(11):2987-3001.
8. Chalut KJ, Paluch EK. The actin cortex: a bridge between cell shape and function. Dev Cell. 2016;38(6):571-573.
9. Bhatlekar S, Manne BK, Basak I, et al. miR-125a-5p regulates megakaryocyte proplatelet formation via the actin-bundling protein L-plastin. Blood. 2020;136(15):1760-1772.
10. Schachtner H, Calaminus SD, Sinclair A, et al. Megakaryocytes assemble podosomes that degrade matrix and protrude through basement membrane. Blood. 2013;121(13):2542-2552.
11. Chen H, Mocsai A, Zhang H, et al. Role for plastin in host defense distinguishes integrin signaling from cell adhesion and spreading. Immunity. 2003;19(1):95-104.
12. Morley SC. The actin-bundling protein L-plastin supports T-cell motility and activation. Immunol Rev. 2013;256(1):48-62.
13. Fritzsche M, Thorogate R, Charras G. Quantitative analysis of ezrin turnover dynamics in the actin cortex. Biophys J. 2014;106(2):343-353.
14. Evans E, Heinrich V, Leung A, Kinoshita K. Nano- to microscale dynamics of P-selectin detachment from leukocyte interfaces. I. Membrane separation from the cytoskeleton. Biophys J. 2005;88(3):2288-2298.
15. Heinrich V, Leung A, Evans E. Nano- to microscale dynamics of P-selectin detachment from leukocyte interfaces. II. Tether flow terminated by P-selectin dissociation from PSGL-1. Biophys J. 2005;88(3):2299-2308.
16. Bury L, Falcinelli E, Gresele P. Learning the ropes of platelet count regulation: inherited thrombocytopenias. J Clin Med. 2021;10(3):533.
17. Chang Y, Auradé F, Larbret F, et al Proplatelet formation is regulated by the Rho/ROCK pathway. Blood. 2007;109(10):4229-4236.
18. Bisaria A, Hayer A, Garbett D, Cohen D, Meyer T. Membrane-proximal F-actin restricts local membrane protrusions and directs cell migration. Science. 2020;368(6496):1205-1210.